PORE STRUCTURE AND GRAPHITIC SURFACE ORDER OF MESOPOROUS CARBON MOLECULAR SIEVES BY LOW-PRESSURE NITROGEN ADSORPTION

H. Darmstadt[1], C. Roy[1], S. Kaliaguine[1], S.J. Choi[2] and R. Ryoo[2]
[1] Chemical Engineering Department, Laval University
Québec, Qc, G1K 7P4, Canada, E-mail: darmstad@gch.ulaval.ca
[2] Department of Chemistry (School of Molecular Science-BK21)
Korea Advanced Institute of Science and Technology
Taejon, 305-701, Korea, E-mail: rryoo@mail.kaist.ac.kr

Introduction

Porous carbons such as activated carbons, are important adsorbents and catalyst supports. Activated carbons are produced from various carbon-containing materials by pyrolysis/carbonisation, followed by partial oxidation (activation). The pore structure of the activated carbons can be controlled to a certain degree by the carbonisation and activation conditions. However, their pore size distribution is usually relatively wide and it is not possible to produce activated carbons which have predominately narrow mesopores [1,2]. Such materials are highly desirable for the adsorption and catalytic transformation of large molecules. A different synthesis approach is to perform the pyrolysis/carbonisation in a suitable matrix such as microporous zeolites [3-5] or mesoporous silicas [6]. Obviously, the structure of the produced carbon will be controlled by the pore structure of the matrix. In a second step of the synthesis, the carbon is liberated by removal of the matrix, for example by treatment with hydrofluoric acid in the case of zeolite or silica matrices. The carbon sieves obtained by this method usually have a narrow pore size distribution. A large-scale production of mesoporous carbons by this approach should be possible since a convenient synthesis method for suitable mesoporous silicas was recently developed [7,8].

In the present work the effect of a heat-treatment on the pore structure of mesoporous carbon sieves produced in a MCM-48 and SBA-15 silica matrix, respectively, was investigated by nitrogen adsorption at -196 °C over a wide pressure range. The nitrogen adsorption data also contain information on the graphitic order of the mesopore surface. The graphitic order of this internal surface was compared to the structure of the outer surface as studied by secondary ion mass spectroscopy (SIMS).

Experimental Details

Materials

Mesoporous carbon molecular sieves were produced by pyrolysis of sucrose adsorbed in a MCM-48 [7] and a SBA-15 [9] silica matrix, respectively. Different pyrolysis experiments were performed at temperatures ranging from 700 to 1100 ºC. Then, the mesoporous carbon sieves were liberated by dissolving the silica matrix in hydrofluoric acid solution. Some samples were subsequently heat-treated at temperatures ranging from 1100 to 1600 ºC. The synthesis conditions of the mesoporous carbons are summarised in Table 1. A non-porous thermal carbon black (SC N990) and a predominately microporous activated carbon (Calgon F-300) were used as reference compounds. Information on the surface morphology and chemistry of the reference compounds can be found elsewhere [10-12].

Nitrogen adsorption

An Autosorb-1 MP apparatus from Quantachrome, Boynton Beach, FL, USA, was used for the nitrogen adsorption experiments at -196 °C. Prior to the adsorption experiment, samples of approximately 25 mg carbon sieve were outgassed at 200 ºC until the pressure increase in the closed sample cell was lower than 1.3 Pa/min. A typical fi-

Table 1, Synthesis parameter of the mesoporous carbon molecular sieves

Sample	Silica matrix	Pyrolysis temperature [°C]	Post-pyrolysis heat-treatment temperature [°C]
CMK-3F(A)	SBA-15	700	-
CMK-3F(B)	SBA-15	900	-
CMK-3F(C)	SBA-15	900	1100[a]
CMK-3F(D)	SBA-15	900	1300[b]
CMK-3F(E)	SBA-15	900	1600[b]
CMK-1F(A)	MCM-48	700	-
CMK-1F(B)	MCM-48	900	-
CMK-1F(C)	MCM-48	900	1100[a]
CMK-1F(D)	MCM-48	1100	-
CMK-1F(E)	MCM-48	900	1300[b]
CMK-1F(F)	MCM-48	900	1600[b]

[a] Under vacuum

[b] Under nitrogen

nal dynamic pressure was 0.13 Pa. The BET equation [13] was used to calculate the apparent surface area from P/P_0 data between 0.05 and 0.15. The cross sectional area of the nitrogen molecule was assumed to be 16.2 Å². The mesopore size distribution and the mesopore volume were calculated by the BJH method [14] using desorption data. It should be mentioned that the mesopores of the carbon sieves produced in the MCM-48 matrix were approximately 20 to 25 Å wide. The application of the BJH method to the adsorption data of materials with such narrow mesopores limits the precision of the results. Therefore, the widths of the mesopores of the carbon sieves produced in a MCM-48 matrix were only discussed qualitatively. However, the trends in pore width indicated by the BJH results were confirmed by results from the adsorption potential distribution (APD). The combined volume of micro and mesopores was calculated from the amount of nitrogen adsorbed at $P/P_0 = 0.95$ [15]. This calculation slightly overestimates the pore volume since at $P/P_0 = 0.95$ a certain amount of nitrogen is also adsorbed on the outer surface. The nitrogen adsorption data were also used to calculate the adsorption potential distribution (APD). The adsorption potential (A) is defined as the negative change of the Gibbs free energy of adsorption:

$$A = - \Delta G = - RT \ln (P/P_0) \quad (1)$$

where R is the gas constant, T is the absolute temperature and P/P_0 is the relative pressure [16]. The APD was normalised to the monolayer volume:

$$APD = (\Delta V / V_{Monolayer}) / \Delta A \quad (2)$$

where ΔV and ΔA are the differences in volume of adsorbed gaseous nitrogen [cm³ STP/ g] and in the adsorption potential, respectively, between two neighbouring points of the adsorption isotherm and $V_{Monolayer}$ is the monolayer volume, calculated from the APD (see below).

Results and Discussion

Nitrogen adsorption isotherms of carbon sieves produced in a SBA-15 matrix

The nitrogen adsorption isotherms of mesoporous carbon molecular sieves produced in MCM-48 [17] and SBA-15 [9] silica matrices, respectively, have already been described elsewhere. Briefly, the observed steep increase in adsorption on the carbons produced in a SBA-15 matrix (series CMK-3F, see Table 1) for relative pressures (P/P_0) from 0.4 to 0.8 and the corresponding hysteresis loop are typical for materials with narrow mesopores. The small adsorption for P/P_0 above 0.95, where multilayer formation takes place, indicates a small outer surface. It was furthermore concluded from nitrogen adsorption data that the non heat-treated carbon sieves contain micropores [9,17].

In the present investigation, it was observed that for carbon sieves produced in a SBA-15 matrix the isotherms changed considerably upon heat-treatment. First, the adsorption decreased with increasing heat-treatment temperature. This decrease was especially pronounced for very low relative pressures ($P/P_0 < 0.02$), whereas for higher P/P_0 the decrease was smaller (Fig. 1). This is a first indication that during the heat-treatment mostly micropores were "lost", whereas the volume of mesopores only changed little. Changes were also observed for the shape of the low-pressure portion of the isotherms, especially after heat-treatment at 1600 °C (sample CMK-3F(E), Fig. 2). The shape of the low-pressure portion of the isotherm depends on the microporosity and graphitic order of the carbon surface [10,16,18]. The temperature dependence of these two properties will be discussed in detail below.

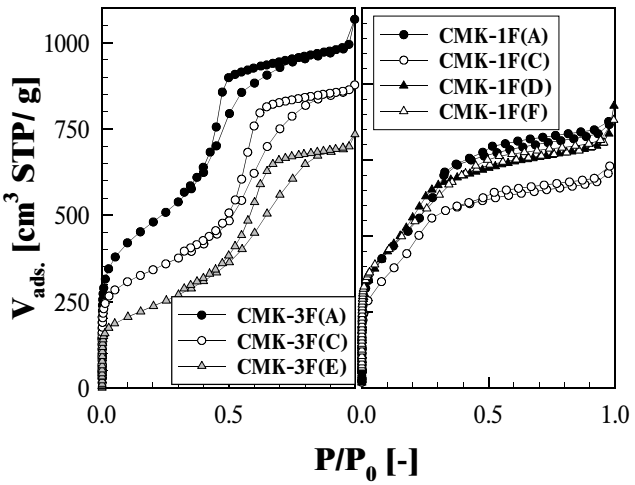

Fig. 1 Nitrogen adsorption isotherms at -196 °C for heat-treated carbon sieves produced in a SBA-15 (series CMK-3F) and MCM-48 (series CMK-1F) silica matrix, respectively.

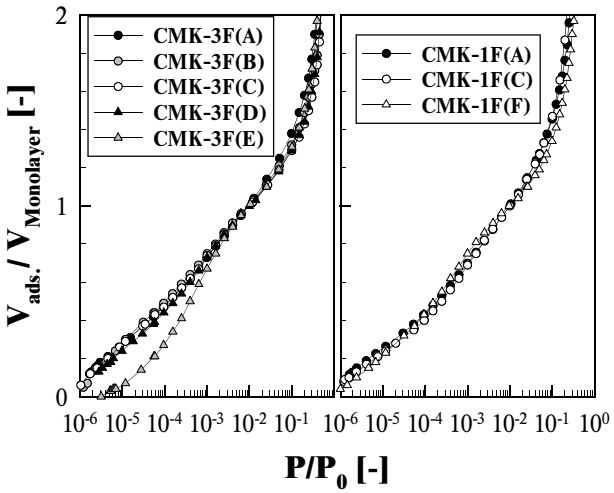

Fig. 2 Low-pressure nitrogen adsorption isotherms for heat-treated carbon sieves produced in a SBA-15 (series CMK-3F) and MCM-48 (series CMK-1F) silica matrix; normalised to the monolayer volume

The second change of the isotherms was that the hysteresis loop was shifted to higher P/P_0 with increasing heat-treatment temperature (Fig. 1). This shift indicates that the width of the mesopores increased during the heat-treatment. A widening of the mesopores was confirmed by the mesopore size distribution calculated by the BJH method. The maximum of the mesopore size distribution shifted from approximately 35 Å (CMK-3F(A)) to 50 Å (CMK-3F(E)). Furthermore, the mesopore size distribution became wider (Fig. 3). According to the BJH pore size distribution there were only weak contributions of mesopores wider than 80 Å (not shown). The significant changes of the pore structure had a limited influence on the volume of the small mesopores (width from 20 to 80 Å). Up to a heat-treatment temperature of 1300 °C (sample CMK-3F(D)) the volume of the narrow mesopores decreased from 1.18 to 1.16 cm³/g. Only when the temperature was further raised to 1600 °C (sample CMK-3F(E)) the volume of the narrow mesopores decreased significantly to 0.98 cm³/g (Table 2).

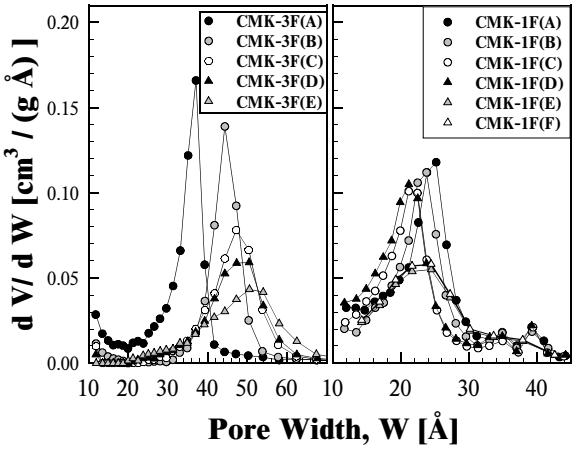

Fig. 3 Mesopore size distributions of heat-treated carbon sieves produced in a SBA-15 and a MCM-48 silica matrix, respectively; BJH method.

Nitrogen adsorption isotherms of carbon sieves produced in a MCM-48 matrix

As for the samples discussed above, carbon sieves produced in a MCM-48 matrix have a mixed micro/mesoporous structure. However, the isotherms of the carbon sieves produced in a MCM-48 matrix (series CMK-1F) and SBA-15 matrix (series CMK-3F) differ considerably [17]. The adsorption on the non heat-treated carbon sieve produced in the MCM-48 matrix was notably lower as compared to the corresponding sample produced in the SBA-15 matrix (Fig. 1). Furthermore, for the carbons produced in a MCM-48 matrix, the step increase in adsorption due to filling of mesopores occurred at lower pressures as compared to carbon sieves produced in the SBA-15 matrix. This suggests that the mesopores in the carbons produced in the MCM-48 matrix were narrower as compared to the carbons produced in a SBA-15 matrix. This may be related to differences in the behaviour of the two carbon materials upon removal of the silica matrix. During this treatment, the carbon sieves produced in a MCM-48 matrix undergo a transformation into a new structure, whereas the carbons produced in a SBA-15 matrix retain the structure of the silica pore system [9].

The data of the present investigation also show that the effect of the heat-treatment was different for the carbons produced in the two matrices. First, the changes of the isotherm upon heat-treatment were less pronounced for the

Table 2, Surface area, pore volumes and pore width of mesoporous carbon molecular sieves

Sample	Specific surface area [m²/g]		Mesopore width [a]	Pore volume [cm³/g]		
				Mesopores		Micro+mesopores
	BET	APD [b]	[Å]	20-80 Å	20-500 Å	$P/P_0 = 0.95$
CMK-3F(A)	1721	(1322) [c]	35.0	1.18	1.25	1.53
CMK-3F(B)	1322	1080	44.5	1.16	1.23	1.42
CMK-3F(C)	1218	1040	47.0	1.04	1.18	1.34
CMK-3F(D)	1200	1018	49.0	1.16	1.23	1.36
CMK-3F(E)	837	727	50.5	0.98	1.04	1.15
CMK-1F(A)	1908	(1344) [c]	25.0	-	-	1.31
CMK-1F(B)	1683	(1083) [c]	24.0	-	-	1.16
CMK-1F(C)	1683	1102	21.0	-	-	1.07
CMK-1F(D)	1968	1344	21.0	-	-	1.26
CMK-1F(E)	1680	1326	24.5	-	-	1.07
CMK-1F(F)	1896	1473	24.5	-	-	1.26

[a] Maximum in the BJH pore size distribution

[b] Adsorption potential distribution, see text for details

[c] Approximation, see text for details

carbon sieves produced in the MCM-48 matrix as compared to the carbons produced in the SBA-15 matrix. Furthermore, with increasing heat-treatment temperature there was a steady decrease in the amount adsorbed and a steady shift of the hysteresis to higher pressures for the carbons produced in the SBA-15 matrix. On the other hand, for the carbons produced in the MCM-48 matrix with increasing heat-treatment temperature first the amount adsorbed decreased (samples CMK-1F(A) > CMK-1F(B) > CMK-1F(C)) and then increased again (samples CMK-1F(C) ~ CMK-1F(E) < CMK-1F(F)). A similar temperature dependence was observed for the width of the mesopores. According to the BJH pore size distribution, upon heating the width of the mesopores first decreased from approximately 25 Å (sample CMK-1F(A), 700 °C) to 21 Å (samples CMK-1F(C) and CMK-1F(D), 1100 °C). Upon further temperature increase, the pore size distribution became wider and the maximum was shifted to approximately 24.5 Å (Fig. 3). As for the carbon sieves produced in a SBA-15 matrix, the BJH pore size distribution indicated only a weak contribution of mesopores wider than 80 Å (not shown). It is worth mentioning that the pore widths indicated by the BJH method extended well into the micropore region (width < 20 Å). However, the BJH method normally significantly underestimates the width of mesopores [8]. Thus, the actual mesopore widths are most probably larger as indicated in Fig. 4.

There are also indications that in addition to the heat-treatment temperature, the synthesis procedure also had an important influence on the structure of the carbon sieves. The highest temperature during the synthesis of the two samples CMK-1F(C) and CMK-1F(D) was 1100 °C. However, sample CMK-1F(D) was produced by pyrolysis at this temperature, whereas sample CMK-1F(C) was obtained by pyrolysis at 900 °C and a subsequent heat-treatment at 1100 °C (Table 1). In spite of the same highest temperature encountered by the two samples during their synthesis, there were pronounced differences in their pore structure. The surface area and the pore volume of sample CMK-1F(D) was considerably higher as compared to CMK-1F(C) (Table 2).

Adsorption potential distribution of carbon sieves produced in a SBA-15 matrix

As mentioned above, the nitrogen isotherms indicated that the micropore volume of carbons produced in a SBA-15 matrix decreased upon heat-treatment. For porous carbons, such as activated carbons, the micropore volume can be determined from comparison plots such as t- or α-plots [19]. However, the presence of very narrow mesopores makes the determination of the micropore volume by comparison plots unreliable [17].

Thus, in the present investigation information on the development of the microporosity upon heat-treatment is extracted from the adsorption potential distribution (APD). The APD of carbon materials is influenced by the porosity and the structural order of the surface. As the easier case,

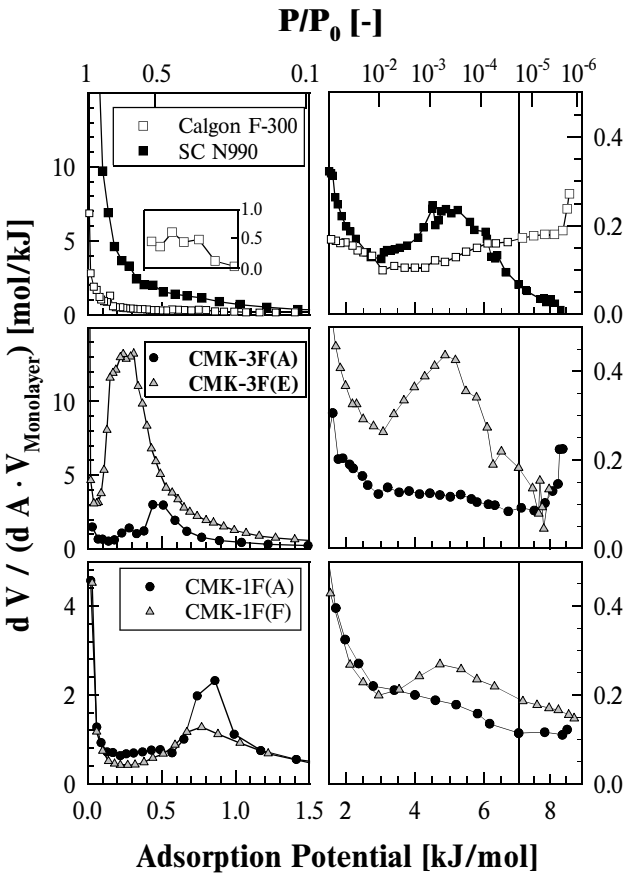

Fig. 4 Adsorption potential distributions for mesoporous carbon sieves, non-porous carbon black SC N990 and predominant microporous activated carbon (Calgon F300); normalised to the monolayer volume.

first the APD of non-porous carbons is discussed. The APD of graphitized carbon blacks show peaks at approximately 5.5, 3.0, and 0.7 kJ/mol [18]. These signals are attributed to the formation of the nitrogen monolayer, to a two-dimensional fluid-solid transition and to the second layer formation, respectively. With decreasing graphitic order of the carbon surface these peaks become wider and were shifted to lower adsorption potentials. Finally, the peaks for two-dimensional fluid-solid transition and the second-layer formation are disappearing. Thus, the APD of non-graphitized carbon blacks only shows a monolayer formation peak at 5.5 to 3.3 kJ/mol, depending on the graphitic order of the surface [10]. As an example the APD of the non-graphitized thermal carbon black SC N990 is presented in Figure 4. The APD of this sample showed a monolayer formation peak at approximately 5.0 kJ/mol. Because of the relatively low graphitic order, the APD showed no indication of a two-dimensional fluid-solid transition or a second-layer formation peak.

The presence of pores causes the appearance of additional peaks in the APD. In carbons the filling of very narrow

micropores (width < 9 Å) occurs in one step, whereas in larger micro and mesopores first a monolayer and then, depending on the pore size, additional layers are formed before the pores are filled [20]. Consequently, in the APD of carbons with very narrow micropores a one-step micropore filling peak is observed [21]. The one-step filling of the small micropores (width < 9 Å) occurs at relative pressures below approximately 10^{-4} [20]. This pressure corresponds to an adsorption potential of approximately 6.0 kJ/mol. Consequently, in the APD the peak for one-step filling of narrow micropores is located at adsorption potentials above 6.0 kJ/mol. For carbons with pores wider than 9 Å a monolayer formation and a secondary pore filling peak are observed in the APD. Depending on the size of the pores, these two peaks may overlap.

As an example for a predominately microporous activated carbon, the APD of Calgon F-300 is presented in Figure 4. The APD showed a strong signal above an adsorption potential of 8.5 kJ/mol, indicating the presence of narrow micropores. The shoulder located between adsorption potentials of approximately 5 to 8.5 kJ/mol most probably contains contributions from the monolayer formation and secondary pore filling. Furthermore, there was a very weak peak at adsorption potentials between approximately 0.5 to 0.9 kJ/mol (Inset in Figure 4) which indicates a small concentration of mesopores.

The discussion of the APD of the two reference compounds allows information to be obtained on the pore structure of the carbon sieves from their APD. The APD of sample CMK-3F(A) produced at 700 °C showed a strong signal at an adsorption potential of approximately 8.5 kJ/mol (Fig. 4). This is a clear indication for the presence of narrow micropores. The peak at approximately 0.5 kJ/mol is due to mesopore filling. The heat-treatment had a significant influence on the APD of the carbon sieves. In the APD of sample CMK-3F(E), heat-treated at 1600 °C, no signals due to small micropores were found at adsorption potentials above 6 kJ/mol. Instead, the APD approached zero for higher adsorption potentials.

For adsorption potentials above 2 kJ/mol the APD of the carbon sieve resembled those of the non-porous carbon black SC N990. As for the carbon black, a pronounced peak at approximately 5 kJ/mol was observed. Theoretically, this peak could be assigned to larger micropores or the formation of the nitrogen monolayer. However, the creation of micropores during heat-treatment in nitrogen atmosphere or under vacuum is very unlikely. As discussed below, there are additional observations which indicate that during the heat-treatment no micropores were formed. The micropore volume can be estimated from the difference of the combined volume of the meso and micropores (calculated from the amount of nitrogen adsorbed at $P/P_0 = 0.95$) and the BJH mesopore volume (Table 2). These data indicate that the micropore volume of the carbon sieves strongly decreased during the heat-treatment. On the other hand, it is reasonable to assume that the heat-treatment increased the structural order of the surface. As discussed above, the APD of carbons with a certain order shows a monolayer formation peak. The peak at 5 kJ/mol was, therefore, assigned to the monolayer formation.

Another effect of the heat-treatment on the APD was that the mesopore filling peak was shifted to lower adsorption potentials, which reflects the widening of the mesopores, already observed in the BJH pore size distribution (Fig. 3). It can be concluded that upon heat-treatment of the carbon sieves produced in a SBA-15 matrix the initially present narrow micropores disappeared, whereas the mesopores became wider.

Adsorption potential distribution of carbon sieves produced in a MCM-48 matrix

As for the non heat-treated carbon sieve produced in a SBA-15 matrix (CMK-3F(A)), the APD of the corresponding carbon sieve produced in a MCM-48 matrix (CMK-1F(A)) showed a strong signal at adsorption potentials above 6 kJ/mol (Fig. 4). This indicates that both samples contained narrow micropores. The effect of the heat-treatment on the narrow micropores, however, was different. For the carbons produced in a SBA-15 matrix, the volume of the micropores decreased upon heat-treatment. Finally, after treatment at 1600 °C (nearly) all micropores have disappeared (see above). However, in all APD of the heat-treated carbon sieves produced in a MCM-48 matrix strong signals were observed for adsorption potentials above 6 kJ/mol (only shown for sample CMK-1F(F) in Fig. 4). Thus, for these carbons, the narrow micropores did not disappear upon heat-treatment. Even after a heat-treatment temperature of 1600 °C the carbon sieve still contained a significant concentration of narrow micropores. This conclusion is supported by the observation that for very low P/P_0 the adsorption on the sample CMK-1F(A) (non heat-treated) and on sample CMK-1F(F) (treated at 1600 °C) were very similar (Fig. 1).

As mentioned above, for the carbon sieves produced in a SBA-15 matrix, the micropore volume can be estimated by the difference of the nitrogen volume adsorbed at a relative pressure of 0.95 and the mesopore volume determined by the BJH method (Table 2). Unfortunately, this was not possible for the carbon sieves produced in a MCM-48 matrix. For the narrow mesopores of these materials the pore volume cannot be reliably calculated by the BJH method.

For the carbon sieves discussed here, the density functional theory (DFT) method is also not suitable since it assumes slit-like pores [22]. This may be a valid assumption for the micropores. The shape of the mesopores in the carbon sieves, however, most likely correspond to the volume occupied by the silicon and oxygen atoms of the silica matrix and may be described as a three-dimensional network of roughly cylindrical pores. Because of the presence of both slit-like and cylindrical pores, models which are based on exclusively cylindrical pores [23] are also not applicable.

Graphitic surface order of the surface of carbon sieves

Information on the graphic order of the surface can be ob-

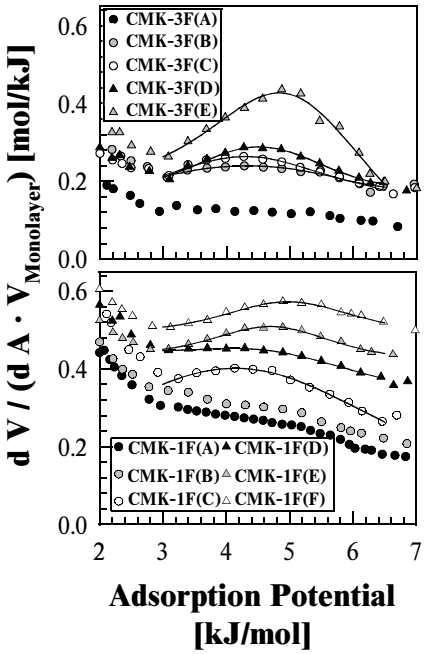

Fig. 5 Adsorption potential distribution for mesoporous carbon sieves, monolayer formation peak

tained from the monolayer formation peak. As mentioned above, the position of the monolayer formation peak depends on the graphitic order of the carbon surface. For a series of graphitized carbon blacks a correlation between the bulk graphitic order, determined by X-ray diffraction, and the position of the monolayer formation peak was observed. With increasing graphitic order the monolayer formation peak was shifted to higher adsorption potentials [18].

It is reasonable to assume that during the heat-treatment the order of the carbon surface increases. Thus, upon heat-treatment, the monolayer formation peak in the APD is expected to be shifted to higher adsorption potentials. Exactly this behaviour was observed in the present work for both series of heat-treated carbon sieves (Fig. 5). The APD of the carbon sieve produced in the SBA-15 matrix at 700 °C (sample CMK-3F(A)) showed no monolayer formation peak. However, after heating to 900 °C (CMK-3F(B)) a weak peak appeared at approximately 4.3 kJ/mol. Upon further heating the monolayer formation peak became more pronounced and was shifted to higher adsorption potentials. After heat-treatment at 1600 °C, the peak was located at an adsorption potential of approximately 5.0 kJ/mol (sample CMK-3F(E)).

For the carbon sieves produced in a MCM-48 matrix a similar temperature dependence of the position of the monolayer formation peak was observed. In fact, considering the uncertainty of the determination of the position of the rather wide monolayer formation peaks, the temperature dependence of the peak position was practically the same for the two series (Fig. 6). Since the pore structure of the carbons produced in the two matrices differed considerably, this suggests that graphitic order depends on the heat-treatment temperature and not or only very little on the pore structure.

During adsorption, the nitrogen monolayer is formed in the mesopores and on the outer surface of the carbon particles. However, as already mentioned, for the carbon sieves the outer surface was very small as compared to the mesopore surface. Thus, the position of the monolayer formation peak depends essentially on the order of the mesopore surface. It should be mentioned that the mesostructured carbons reported here constitute a very special case where the order of an internal surface can be studied by nitrogen adsorption. For the samples studied, the monolayer formation peak extended from adsorption potentials of approximately 3 to 6 kJ/mol (Fig. 5), corresponding to a P/P_0 range of approximately 10^{-4} to 10^{-2}. At these pressures, when present, pores with widths between 9 and 12 Å are filled [20]. Only for carbons where the volume of such pores is very low, the monolayer formation in larger pores and the outer surface does not overlap with pore filling. Consequently, only for such carbons can one obtain information on the surface order from the nitrogen isotherms. Furthermore, if one is interested in properties of the mesopore surface the outer surface has to be small as compared to the surface of the mesopores. Unfortunately, these conditions are not met by most porous carbons. These materials usually contain micropores with widths between 9 and 12 Å. Thus, the analysis based on the low-pressure nitrogen isotherm presented here cannot be applied to "usual" porous carbons.

Comparison with surface spectroscopic results

It was outlined in the previous paragraph that for the samples studied it was possible to obtain information on the order of the mesopore surface from the low-pressure nitrogen adsorption data. In a parallel work [24], the polyaromatic character of the outer surface of the carbon sieves was studied by secondary ion mass spectroscopy (SIMS). Briefly, in the SIMS experiment the sample surface is bombarded with high-energy ions, causing the ejection of ions from the surface. Which ions are ejected depends on the chemical nature of the surface. The SIMS spectra of the negative ions showed intense C_2H^- and C_2^- peaks. The most important contribution to the C_2H^- peak arises from the edge of a polyaromatic system, whereas most of the C_2^- ions originate from the interior of the polyaromatic system [11,25-27]. A small C_2H^-/C_2^- ratio therefore indicates a large poly-aromatic, graphite-like order of the outer surface.

In Figure 6 the SIMS C_2H^-/C_2^- ratio and the position of the monolayer formation peak in the APD, the two measures for the order of the mesopore and outer surface, are plotted as a function of the heat-treatment temperature. Both the polyaromatic order of the outer surface and the order of the mesopore surface increased during the heat treatment. However, the temperature dependence of the two properties was not the same. The SIMS data indicated that the

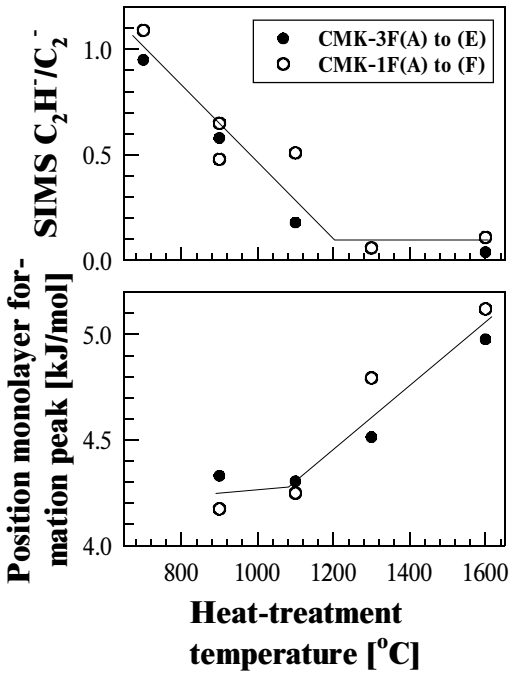

Fig. 6 SIMS C_2H^-/C_2^- ratio (measure for the polyaromatic character of the outer surface) and position of the monolayer formation peak (measure for the order of the mesopore surface) as a function of the heat-treatment temperature

polyaromatic character of the outer surface strongly increased up to a temperature of approximately 1200 °C. A further increase of the temperature only had a limited effect. The situation was different for the order of the mesopore surface. Below 1100 °C there were only little changes, whereas the order of the mesopore surface strongly increased for higher temperatures. The observation that considerably higher temperatures are necessary to change the order of the internal mesopore surface as compared to the outer surface may be explained as follows. In the non heat-treated carbon sieves the mesopore system corresponds to the space initially occupied by the silicon and oxygen atoms of the silica matrix. Such a three-dimensional carbon structure is relatively rigid and changes in the arrangement of the carbon atoms require much higher energies (temperatures) as compared to the less-constrained outer surface. However, it is also possible that the differences between the outer and internal surface are related to the fact that during the removal of the silica matrix with hydrofluoric acid first the outer carbon surface and later the surface in the interior of the carbon particles was liberated. Thus, the outer surface was in contact with the hydrofluoric acid longer as compared to the internal mesopore surface, which may have influenced the reactivity of the carbon surface. It can be concluded that in addition to the pore structure also the surface order changes during the heat-treatment. Both properties will influence the adsorption behaviour of the carbon sieves.

Specific surface area of carbon sieves

The specific surface areas of the mesoporous carbon molecular sieves determined by the BET method were very large. BET surface areas of up to 1721 m²/g were found (Table 2). Considering that the theoretical surface area of a single graphite layer is approximately 1800 m²/g [28], the BET surface areas for the carbon sieves are unrealistically high. The BET model does not consider adsorption in pores. It is well-known that the BET model therefore often significantly overestimates the surface area of porous solids.

A more realistic value for the specific surface area can be obtained from the adsorption potential distribution (APD). For most of the samples studied, the APD showed a monolayer formation peak. The low adsorption potential end of the monolayer formation peak (minimum in the APD) indicates the point where the monolayer has been completed. From this point the volume of the nitrogen monolayer and the specific surface area can be calculated [16]. For the samples studied, the low adsorption potential end of the monolayer formation peak was located at an adsorption potential of approximately 3 kJ/mol (Fig. 5). This adsorption potential corresponds to a P/P_0 of approximately 10^{-2}. Thus, the amount of nitrogen adsorbed at $P/P_0 = 10^{-2}$ was assumed to be the monolayer. The specific surface area was calculated from this amount. These APD surface areas were considerably lower compared to the BET surface areas (Table 2) which is more realistic for predominantly mesoporous carbons. However, even the lower APD values indicate that the carbon sieves have the high surface areas required by a "good" adsorbent.

It should be mentioned, that there is some uncertainty in the determination of the end of the monolayer formation peak and consequently in the determination of the APD surface area. However, for activated carbons the agreement between the surface areas calculated from the APD and by the DFT method was found to be usually better than 10 % [16].

In the present work, for some samples (CMK-3F(A), CMK-1F(A) and CMK-1F(B)), no monolayer formation peak was observed. Therefore for these samples the APD surface area is only an approximation.

Conclusions

Carbon sieves produced in SBA-15 and MCM-48 silica matrices are predominantly mesoporous. However, the materials also contain narrow micropores (width < 9Å). For the carbon sieves produced in SBA-15 matrix, upon heating the concentration of micropores decreases until at a temperature of 1600 °C a purely mesoporous material is obtained. Furthermore, the mesopore diameter increases from 35 to 50 Å. These changes can be explained as follows. The structure of the carbon corresponds to the three dimensional pore system of the SBA-15 silica, which may be visualised as interconnected carbon rods. During the

heat-treatment, the carbon rods are shrinking and voids in the rods - the micropores - are disappearing. As the carbon rods become narrower, the space between them - the mesopores - becomes wider. The situation is different for the carbon sieves produced in a MCM-48 matrix. These materials contain, in addition to narrow micropores, small mesopores (width ~ 25Å). Upon heat-treatment the width of the mesopores first decreases and then increases again. The narrow micropores do not disappear during the heat-treatment.

The carbon sieves have mesopore volumes and BET surface areas of up to 1.25 cm^3/g and 1721 m^2/g, respectively. Even if the BET surface areas are overestimated, the lower, but more realistic, surface areas calculated from the adsorption potential distributions (APD) of approximately 730 to 1400 m^2/g indicate that these materials have a high potential as adsorbents for large molecules and as catalyst support. It should also be advantageous that for carbon sieves produced in a SBA-15 matrix the concentration of micropores can be regulated by the heat treatment temperature.

The structural order of the outer and of the mesopore surface increases upon heat-treatment. However, changes of the mesopore surface occur at higher temperatures as compared to the outer surface. In spite of the different structure of the carbon sieves produced in the two matrices, for a given temperature the structural order of the outer and mesopores surface, respectively, was similar.

References

[1] Bansal RC, Donnet J-B and Stoeckli F. In: Active Carbon, New York, USA, Marcel Dekker Inc. 1988, pp. 1.

[2] Jankowska H, Swiatkowski A and Choma J. In: Active Carbon, Cichester, UK, Ellis Horwood 1991, pp. 75.

[3] Kyotani T, Nagai T, Inoue S and Tomita A. Formation of New Type of Porous Carbon by Carbonization in Nanochannels in Zeolite. Chem. Mater. 1997; 9: 609-615.

[4] Johnson SA, Brigham ES, Olivier PJ and Mallouk TE. Effect of Micropore Topology on the Structure and Properties of Zeolite Polymer Replicas. Chem. Mater. 1997; 9: 2448-2458.

[5] Rodriguez-Mirasol J, Cordero T, Radovic LR and Rodriguez JJ. Structural and Textural Properties of Pyrolytic Carbon Formed within a Microporous Zeolite Template. Chem. Mater. 1998; 10: 550-558.

[6] Ryoo R, Joo SH and Jun S. Synthesis of highly ordered carbon molecular sieves via template-mediated structural transformation. J. Phys. Chem. B. 1999; 103: 7743-7746.

[7] Ryoo R, Joo SH and Kim JM. Energetically Favored Formation of MCM-48 from Cationic-Neutral Surfactant Mixtures. J. Phys. Chem. B. 1999; 103: 7435-7440.

[8] Kruk M, Jaroniec M, Ryoo R and Joo SH. Characterization of MCM-48 Silicas with Tailored Pore Sizes Synthesized via a Highly Efficient Procedure. Chem. Mater. 2000; 12: 1414-1421.

[9] Jun S, Joo SH, Ryoo R, Kruk M, Jaroniec M, Liu Z, Ohsuma T and Terasaki O. Synthesis of New Nanoporous Carbon with Hexagonally Ordered Mesostructure, submitted.

[10] Darmstadt H and Roy C. Comparative Investigation of Defects on Carbon Black Surfaces by Nitrogen Adsorption and SIMS. Carbon, in press.

[11] Darmstadt H, Cao N-Z, Pantea DM, Roy C, Sümmchen L, Roland U, Donnet J-B, Wang TK, Peng CH and Donnelly, PJ. Surface activity and chemistry of thermal carbon blacks, Rubber Chem. Technol. 2000; 73: 293-309.

[12] Cao N-Z, Darmstadt H and Roy C. Activated Carbon Produced from Charcoal Obtained by Vacuum Pyrolysis of Softwood Bark Residue, Energy Fuels, submitted.

[13] Brunauer S, Emmet PH and Teller E. Adsorption of Gases in Multimolecular Layers. J. Am. Chem. Soc. 1938; 60: 309-319.

[14] Barrett EP, Joyner LG and Halenda PP. The Determination of Pore Volume and Area Distribution in Porous Substances. I Computation from Nitrogen Isotherms. J. Am. Chem. Soc. 1951; 73: 373-380.

[15] Rodriguez-Reinoso F, Molina-Sabio M and Gonzalez MT. The use of steam and CO_2 as activating agents in the preparation of activated carbons. Carbon 1995; 33: 15-23.

[16] Kruk M, Jaroniec M and Gadkaree KP. Determination of the Specific Surface Area and the Pore Size of Microporous Carbons from Adsorption Potential Distributions. Langmuir 1999; 15: 1442-1448.

[17] Kruk M, Jaroniec M, Ryoo R and Joo SH. Characterization of Ordered Mesoporous Carbons Synthesized Using MCM-48 Silicas as Templates. J. Phys. Chem. B. 2000; 104: 7960-7968.

[18] Kruk M, Li ZJ, Jaroniec M and Betz WR. Nitrogen adsorption study of surface properties of graphitized carbon blacks. Langmuir, 1999; 15: 1435-1441.

[19] Gregg SJ and Sing KSW. In: Adsorption, Surface Area, and Porosity, 2nd Edition, London, UK: Academic Press, 1982.

[20] Setoyama N, Suzuki T and Kaneko K. Simulation study on the relationship between a high resolution alpha(s)-plot and the pore size distribution for activated carbon. Carbon 1998; 36: 1459-1467.

[21] Kruk M, Jaroniec M and Gadkaree KP. Nitrogen adsorption studies of novel synthetic active carbons. J. Colloid Interface Sci. 1997; 192: 250-256.

[22] Olivier JP. Improving the models used for calculating the size distribution of micropore volume of activated carbons from adsorption data. Carbon 1998; 36: 1469-1472.

[23] Saito A and Foley HC. Curvature and parametric sen-

sitivity in models for adsorption in micropores. AIChE J. 1991; 37: 429-436.

[24] Darmstadt H, Roy C, Kaliaguine S, Choi S and Ryoo R. Surface Chemistry of Mesoporous Carbon Molecular Sieves. Carbon 2001, International Conference on Carbon, Lexington, Kentucky, USA July 14-19, 2001.

[25] Albers P, Deller K, Despeyroux BM, Schäfer A, Seibold K. XPS-SIMS Study on the Surface Chemistry of Commercially Available Activated Carbons Used as Catalyst Supports. J. Catal. 1992; 133: 467-478.

[26] Albers P, Deller K, Despeyroux BM, Prescher G, Schäfer A and Seibold K. SIMS/XPS Investigations on Activated Carbon Catalyst Supports. J. Catal. 1994; 150: 368-375.

[27] Darmstadt H, Sümmchen L, Roland U, Roy C, Kaliaguine S and Adnot A. Surface versus Bulk Chemistry of Pyrolytic Carbon Blacks by SIMS and Raman Spectroscopy. Surf Interface Anal. 1997; 25: 245-253.

[28] Byrne JF and Marsh H. In: Porosity in Carbons: Characterization and Applications, edited by J.W. Patrick, Halsted Press, Chichester, UK, 1995, pp. 1.